Biophysical Chemistry 182 (2013) 44–50

Contents lists available at ScienceDirect

Biophysical Chemistry

journal homepage: http://www.elsevier.com/locate/biophyschem

Temperature and pressure dependence of azurin stability as monitored by tryptophan fluorescence and phosphorescence. The case of F29A mutant

Danika Tognotti, Edi Gabellieri *, Elisabetta Morelli, Patrizia Cioni

Istituto di Biofisica, CNR, via G. Moruzzi 1, 56124 Pisa, Italy

HIGHLIGHTS

- Thermodynamic characterization of F29A azurin unfolding induced by pressure.
- The engineered cavity appears filled, at least partially, with water molecules.
- Pressure decreases F29A flexibility at high temperature.
- Protein hydration dominates on compaction at lower temperatures.
- The position of the engineered cavity is not a key factor for protein stability.

GRAPHICAL ABSTRACT

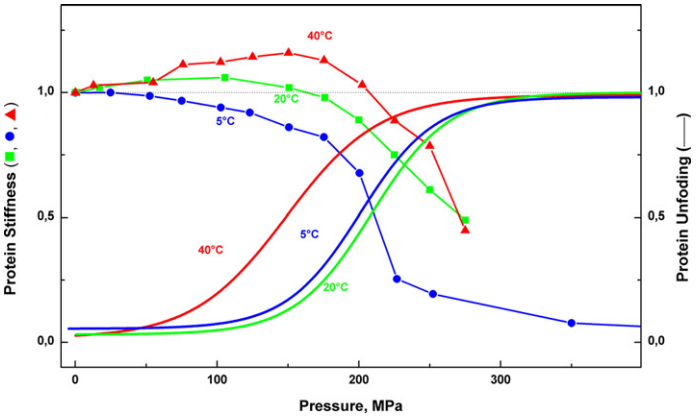

ARTICLE INFO

Article history:
Received 22 April 2013
Received in revised form 7 June 2013
Accepted 7 June 2013
Available online 15 June 2013

Keywords:
High pressure
Protein unfolding
Protein dynamics
Azurin
Tryptophan phosphorescence
Tryptophan fluorescence

ABSTRACT

The effects of a single-point, F29A, cavity-forming mutation on the unfolding thermodynamic parameters of azurin from *Pseudomonas aeruginosa* and on the internal dynamics of the protein fold under pressure were probed by the fluorescence and phosphorescence emission of Trp48, deeply buried in the compact hydrophobic core of the macromolecule.

Pressure-induced unfolding, monitored by the shift in the fluorescence spectrum, led to a volume change of 70–90 ml mol^{-1}. The difference in the unfolding volume between F29A and wild type azurin was smaller than the volume of the space theoretically created in the mutant, indicating that the cavity is, at least partially, filled with water molecules. The complex temperature dependence of the unfolding volume, for temperatures up to 20 °C, suggests the formation of an expanded form of the protein and highlights how the packing efficiency of azurin appears to contribute to the magnitude of internal void volume at any given temperature. Changes in flexibility of the protein matrix around the chromophore were monitored by the intrinsic phosphorescence lifetime. At 40 °C the application of pressure in the predenaturation range initially decreases the internal flexibility of azurin, the trend eventually reverting on approaching unfolding. The main difference between wild type and the cavity mutant is the inversion point which happens at 300 MPa for wild type and at 150 MPa for F29A. This suggests that, for the cavity mutant, pressure-induced internal hydration is more dominant than any compaction of the globular fold at relatively low pressures.

* Corresponding author. Tel.: +39 050 6213048; fax: +39 050 6212760.
E-mail addresses: danika.tognotti@pi.ibf.cnr.it (D. Tognotti), edi.gabellieri@pi.ibf.cnr.it (E. Gabellieri), elisabetta.morelli@pi.ibf.cnr.it (E. Morelli), patrizia.cioni@pi.ibf.cnr.it (P. Cioni).

0301-4622/$ – see front matter
http://dx.doi.org/10.1016/j.bpc.2013.06.005

1. Introduction

Understanding the mechanism underlying pressure-induced protein unfolding should provide more information regarding protein folding, stability and dynamics. It is commonly accepted that water and protein cavities play a fundamental role in this process, however the exact details of pressure unfolding are still under debate. It has been proposed that the mechanism underlying pressure-induced unfolding is the hydration of the protein core [1]. On the other hand, the data obtained by Rouget et al. [2] indicate that exposure of the surface area and the change in hydration are not the main factors responsible for pressure effects on proteins. More recently, Roche et al. [3] presented data suggesting that pressure unfolds proteins primarily because of cavities in the native structure. The authors suggest that the volumetric properties and the responses of proteins to pressure perturbation are determined largely by internal solvent excluded volumes, their anisotropic distribution and their tendency to expand with temperature. The protein interiors are in fact tightly packed, however the packing is not uniform [4]. Packing defects exist ubiquitously in proteins in the form of interior cavities of very different sizes, sometimes as large as 200 $Å^3$, as found by X-ray crystallography [5–8] and by theoretical methods [9–11]. Extensive site-directed mutagenesis experiments have identified that the internal cavities can affect both the biological function [12,13] and structural stability [14–17] of proteins. To determine whether cavities are empty or filled with water is important in clarifying their role in protein denaturation. The extent to which naturally occurring or engineered cavities, sufficiently large to accommodate one or more water molecules, are empty or hydrated depends on several factors (size, hydrophobicity, etc.) and is currently the subject of active debate [18–23]. In addition little is known about how the capacity of the proteins to expand, depending on the strength of the interactions, contributes to the magnitude of the internal void volume at any given temperature. It has also been hypothesized that the contribution of a cavity to the volume difference between the unfolded and folded states depends on the cavity's position within the protein structure, i.e. cavities closer to the surface are likely to contribute less to volume change [24].

In this study we applied high pressure to a cavity-mutant protein, F29A azurin mutant, to examine how a relatively large cavity, created just outside the protein core, could affect both the thermodynamic parameters of pressure unfolding and the pressure modulation of protein dynamics.

Azurin from *Pseudomonas aeruginosa* was chosen as a model system due to the wealth of structural (crystallographic, spectroscopic, and theoretical), thermodynamic, and kinetic data available on both native and mutated forms. Theoretically, the introduction of Ala in place of a bulky Phe creates a cavity of about 100 $Å^3$ per molecule. The mutation makes the protein less stable to guanidinium hydrochloride denaturation [25]. The pressure unfolding equilibrium was monitored by an accompanying large change in the fluorescence spectrum of Trp. On the other hand, the influence of pressure on the dynamics of the protein core was probed by the phosphorescence lifetime of Trp48 [26]. The phosphorescence emission of Trp48 in copper-free azurin is strong and long-lived even in buffer at ambient temperature [27]. This emission has been proved to be remarkably sensitive to the flexibility of the structure surrounding the chromophore induced by a wide range of experimental conditions such as metal binding [27], freezing [28], dehydration [29], high pressure [30], sugar addition [31], and pH [32].

Our results in terms of both stability and flexibility responses to pressure obtained with the single-point mutant, F29A, were similar to those reported for other cavity mutants of azurin where a space is inserted in the inner core of the protein. These findings demonstrate that water molecules do fill the nonpolar cavity of azurin, and suggest that this hydrated cavity leads to the further internal hydration of the macromolecule, thus acting as a nucleation site for unfolding.

2. Materials and methods

All chemicals were of the highest purity grade available from commercial sources and were usually used without further purification. Water, doubly distilled over quartz, was purified by Milli-Q Plus system (Millipore, Bedford, MA). All glassware used for sample preparation was conditioned in advance by standing for 24 h in 10% HCl suprapur (Merck, Darmstadt, Germany). Tris(hydroxymethyl)-aminomethane (Tris) and ethylendiamino-tetracetic acid (EDTA) were from Merck (Darmstadt, Germany). QuickChange kit (Stratagene, LaJolla, CA) was used to construct the F29A mutant of azurin from *P. aeruginosa* [25]. Details about site-directed mutagenesis and protein expression have been previously described [33,34]. Isolation and purification of mutant protein were performed following the procedure described for the native enzyme [35]. Apo-protein was obtained from holo F29A azurin by removing Cu^{++} by potassium cyanide [35].

Before spectroscopic measurements, F29A azurin was extensively dialyzed in 50 mM Tris/1 mM EDTA, pH 7.5. In all experiments, protein concentration was typically 5–10 μM.

2.1. Fluorescence and phosphorescence measurements

Spectroscopic measurements under pressure were carried out by placing the sample cuvette in a pressure cell (SITEC, Zurich, Switzerland) provided with sapphire windows and employing water as pressurizing fluid. Details of the sample cuvette and procedure to avoid leakages between sample and pressurizing fluid during pressure cycles have been reported before [26]. Fluorescence spectra and phosphorescence decays of F29A azurin were monitored at equilibrium as function of pressure, from 0.1 to 650 MPa, at different temperature ranging from −13 to 50 °C. Particular care was taken to assure temperature equilibration of the sample after each pressure variation, which required at least 5 min. The reversibility of the pressure-induced changes in the emission was checked at the end of each pressure cycle.

Measurements were conducted on a homemade apparatus equipped with pulsed excitation (λ_{ex} = 289 nm, pulse duration of 5 ns, pulse frequency up to 10 Hz, and energy per pulse varying from 0.5 to 1 mJ) provided by a frequency-doubled Nd/Yag-pumped dye laser (Quanta Systems, Milan, Italy) [25]. Fluorescence emission collected at 90° from the excitation was monitored by a back-illuminated 1340 × 400 pixels CCD camera (Princeton Instruments Spec-10:400B (XTE), Roper Scientific, Trenton, NJ) cooled to −60 °C. Phosphorescence decays were monitored by collecting the emission at 90° from excitation through a filter combination with a transmission window of 405–445 nm (WG405, Lot-Oriel, Milan Italy; plus interference filter DT-Blau, Balzer, Milan, Italy). The photocurrent amplified by a current-to-voltage converter (SR570, Stanford Research Systems, Stanford, CA) was digitized by a 16 bit speed (1.25 MHz) multi-function data acquisition board (NI 6250 PCI, National Instrument Italy, Milan, Italy) supported by LabVIEW software capable of averaging multiple sweeps. Prompt fluorescence from the same pulse was collected through a 310–375 band pass filter combination (WG305 nm plus Schott UG11) and detected by an ultraviolet-enhanced photodiode (OSD100-7, Centronics, Newbury Park, CA). The prompt fluorescence intensity was used to account for possible variations in the laser output among measurements as well as to obtain fluorescence normalized phosphorescence intensities. All phosphorescence decays were analyzed by a nonlinear least-squares fitting algorithm (DAS6, Fluorescence decay analysis software, Horiba Jobin Yvon, Milan, Italy). For phosphorescence measurements, it is paramount to rid the solution of all O_2 traces. Deoxygenation of protein samples was obtained by adding to the samples, in nitrogen atmosphere, sodium dithionite to get a final concentration of 100 μM [36].

Each spectral and lifetime determination was repeated at least three times.

2.2. Data analysis

Pressure-induced unfolding was analyzed assuming a two-state equilibrium N ↔ U between native (N) and unfolded (U) state with equilibrium constant, K_U, dependent on pressure and temperature. To quantify the unfolding process we used the shift of the intensity-weighted average wavelength, λ_{av}, of the fluorescence spectrum [3]:

$$\lambda_{av} = (\sum \lambda_i F_i)/(\sum F_i) \quad (1)$$

where F_i is the fluorescence intensity at the wavelength λ_i. At pressure p, the intensity-weighted average wavelength, $\lambda_{av(p)}$, is related to the native and unfolded protein fraction by:

$$\lambda_{av(p)} = f_N \cdot \lambda_{av(N)} + f_U \cdot \lambda_{av(U)} \quad (2)$$

where f_N and f_U are the fractions of native and unfolded F29A azurin, and $\lambda_{av(N)}$, $\lambda_{av(U)}$ are their intensity-weighted average wavelengths, respectively. The value of K_U, at each pressure and temperature, was determined experimentally by:

$$K_U = f_U/f_N = f_U/(1-f_U) = \left(\lambda_{av(p)} - \lambda_{av(N)}\right)/\left(\lambda_{av(U)} - \lambda_{av(p)}\right). \quad (3)$$

At selected temperatures, the free energy difference, ΔG, between the unfolded and native state was calculated from K_U as a function of pressure as follows:

$$\Delta G = -RT \ln K_U. \quad (4)$$

As described by Maeno et al. [37], at constant temperature, the second order Taylor expansion of ΔG with respect to p and T may be expressed as:

$$\Delta G = \Delta G_0 + (p-p_0)(\Delta V_0 + \Delta\alpha(T-T_0)) \quad (5)$$

where ΔG_0 and ΔV_0 are the free energy and volume difference between the U and N state at the reference conditions p_0 and T_0, and Δα is the difference in expansivity. Considering:

$$\Delta V = V_U - V_N = (\Delta V_0 + \Delta\alpha(T-T_0)) \quad (6)$$

and combining Eqs. (3)–(6) we obtain:

$$\lambda_{av(p)} = \frac{\left(\lambda_{av(N)} - \lambda_{av(U)}\right)}{1 + \exp -[\Delta G_0 + p(\Delta V)/RT]} + \lambda_{av(U)} \quad (7)$$

that we used to determine ΔG_0 and ΔV parameters associated with the folding–unfolding transition.

Assuming that the heat capacity change, ΔC_p, between unfolded and native state is temperature independent, ΔG depends on temperature as described by the modified Gibbs–Helmhotz equation:

$$\Delta G = \Delta H_m(1-T/T_m) + \Delta C_p[(T-T_m) - T\ln(T/T_m)] \quad (8)$$

where T_m and ΔH_m are the temperature at the midpoint of the unfolding transition and the unfolding enthalpy change at T_m, respectively. At selected pressures, we determined experimentally ΔG as a function of temperature. ΔG values were fitted to Eq. (8) to obtain ΔH_m and T_m for both heat and cold denaturation.

If the pressure dependence of ΔG is taken to the second order, we have the following expression [38]:

$$\begin{aligned}(\Delta G(p,T) = {} & \Delta G_0 - \Delta S_0(T-T_0) + \Delta C_p((T-T_0) - T\ln(T/T_0)) \\ & + \Delta V_0(p-p_0) - (\Delta\beta/2)(p-p_0)^2 + \Delta\alpha(T-T_0)(p-p_0)\end{aligned} \quad (9)$$

where Δβ is the isothermal compressibility change and ΔS_0 is the entropy change at the reference point (p_0 and T_0).

The phosphorescence intensity extrapolated at time zero and normalized by the prompt fluorescence is a direct measure of the native protein fraction because the phosphorescence decay of the unfolded protein fraction falls under the detection limit of the instrument and therefore it does not contribute to the total phosphorescence emission. Consequently, phosphorescence measurements provided an independent method, alternative to the shift of the fluorescence spectrum, to assess the equilibrium constant of the unfolding process.

3. Results

3.1. Trp48 fluorescence changes induced by pressure in F29A azurin

As native copper, in both reduced and oxidized states, quenches both fluorescence and phosphorescence of azurin [27], this report examines apo- (metal-free) F29A azurin.

Fig. 1 shows the fluorescence spectrum of Trp48 of F29A azurin at 20 °C and at atmospheric pressure compared to that measured at 500 MPa. Similar to the wild type (WT) azurin, the F29A fluorescence spectrum showed a very blue fluorescence maximum (λ_{max} = 307.5 nm), due to the highly hydrophobic environment and compact structure around Trp48. At high pressure, the fluorescence maximum shifted to higher wavelength (λ_{max} = 363 nm) whereas the total fluorescence emission, as measured from the spectrum area, remained unchanged within experimental error. The spectroscopic features of the spectrum measured at high pressure are typical of the solvent exposed Trp, indicating that F29A unfolded at high pressure. The spectral changes induced by increasing pressure were quantified by determining the shift in intensity-weighted average wavelength, λ_{av}, as defined by Eq. (1). Fig. 2 shows the change in λ_{av} induced at 20 °C by increasing pressure. The λ_{av} values plotted against pressure described a sharp sigmoid curve with the inflection point located at about 200 MPa. Fitting the curve to Eq. (7) gave a standard Gibbs free energy change (ΔG_0) of 18 kJ mol^{-1} and a volume change of −87 ml mol^{-1}. Compared to WT azurin, the F29A mutant is much less stable against pressure, as the fluorescence spectrum of WT protein at ambient temperature is almost unchanged up to 700 MPa [39].

At 20 °C the unfolding process of F29A azurin can be compared with that of C112S azurin (paper submitted), a mutant unable to bind metal ion. The unfolding of F29A azurin occurred at a lower pressure with a $\Delta\Delta G_0 = \Delta G_0(C112S) - \Delta G_0(F29A) = 28.5 - 18 = 10.5$ kJ mol^{-1} and involved a bigger volume change ($\Delta\Delta V = \Delta V(C112S) - \Delta V(F29A) = (-49.5) - (-87) = 37.5$ ml mol^{-1} or 61 Å^3 per molecule). The ΔΔV value is lower than the expected difference in internal

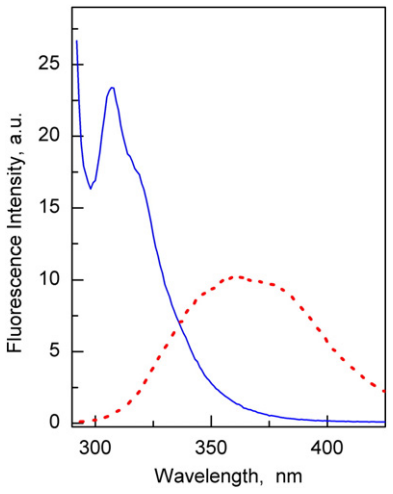

Fig. 1. Fluorescence spectrum of F29A azurin in 50 mM Tris/1 mM EDTA buffer, pH 7.5. Native (solid line), pressure-unfolded (dot line). Spectra were corrected for the instrumental response. Temperature was 20 °C. Excitation wavelength was 289 nm.

void volume of F29A compared to C112S azurin (49 ml mol^{-1} or 82 $Å^3$ per molecule), calculated considering the relative volume of the substituted amino acids [40] and assuming that the protein structure remains unchanged after the substitution.

The unfolding volume of F29A azurin can be compared with both WT and C112S azurin at 40 °C. At this temperature we found a ΔΔV of 17 ml mol^{-1} with respect to WT azurin and 27 ml mol^{-1} with respect to C112S azurin. Again, these values were lower than expected (61 and 49 ml mol^{-1}, respectively), assuming that the amino acid volume remains constant in the 20–40 °C temperature range [41,42].

3.2. Temperature dependence of pressure-induced unfolding of F29A azurin

In order to test how the temperature affects pressure-induced unfolding, we monitored the fluorescence spectrum changes at selected temperatures. At each temperature a sigmoidal transition of λ_{av} was observed. The ΔG_0 and ΔV values calculated according to Eq. (7) are listed in Table 1, along with the pressure at the midpoint of transition, p_m. Protein stability, as estimated from the ΔG_0, decreases with both heating and cooling from room temperature. At each pressure and temperature, we determined the value of ΔG by Eq. (4). We plotted the ΔG values against T (Fig. 3) describing the change in ΔG with temperature at different constant pressures. All curves showed a concave downward curvature and could be fitted reasonably well to the Gibbs–Helmotz equation (Eq. (8)) giving ΔC_p, ΔH_m and T_m parameters for both heat and cold denaturation (Table 2). Although the dependence of ΔV on temperature (Table 1) does not appear to be strictly linear, the relatively large error in the determination of ΔV, especially at low temperatures, and the paucity of the experimental data prevent us from inferring decisively for a non-linear trend. The change in ΔV measured in the temperature range 20–53 °C corresponds to a change in the thermal expansion coefficient (Δα) for unfolding of 0.53 ml mol^{-1} K^{-1}. This value is slightly smaller than those measured in other proteins, such as staphylococcal nuclease (1.33 ml mol^{-1} deg^{-1}) [43], metmyoglobin (1.8 ml mol^{-1} deg^{-1}) [44], ribonuclease A (1.32 ml mol^{-1} deg^{-1}) [45] and hen lysozyme (1.07 ml mol^{-1} deg^{-1}) [37]. The p_m values were fitted versus temperature using Eq. (9), assuming Δβ, Δα and ΔC_p to be temperature independent. From the fitting we derived the change in compressibility on unfolding, $\Delta\beta = -0.05 \pm 0.02$ ml MPa^{-1} mol^{-1}, and an estimate of entropy change, $\Delta S_0 = 263 \pm 11$ J mol^{-1}, at $T_0 = 293$ K and atmospheric pressure (Fig. 4). The enthalpy difference calculated at 20 °C, according to the relationship $\Delta H_0 = \Delta G_0 + T\Delta S_0$, was positive ($\Delta H_0 = 23$ kJ mol^{-1}). From $T_{max} = T_0 - (\Delta H_0 / \Delta C_p)$, we inferred that the temperature of maximum stability of F29A at atmospheric pressure is 13.9 °C.

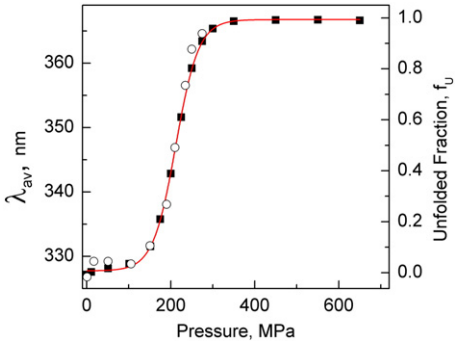

Fig. 2. Intensity-weighted average wavelength of fluorescence spectrum plotted against pressure (black squares). The solid line is the best-fit of experimental data to Eq. (7) and shows the unfolding transition as determined by the fluorescence measurements. The unfolding fraction as estimated from the phosphorescence emission is also shown (open circles). Experimental conditions are as shown in Fig. 1.

Table 1
Temperature dependence of the thermodynamic parameters of pressure unfolding of F29A azurin and its phosphorescence lifetime at atmospheric pressure.

T (K)	ΔG_0 (kJ mol^{-1})[a]	ΔV (ml mol^{-1})[a]	p_m (MPa)[b]	τ (ms)[c]
260	13.4 ± 1.1	−81.2 ± 3.5	165.0	
268	16.0 ± 1.0	−83.5 ± 3.0	191.6	
278	17.2 ± 0.8	−84.4 ± 4.5	203.8	1400 ± 50
283	17.5 ± 0.6	−88.0 ± 2.0	198.9	
293	18.0 ± 0.4	−87.0 ± 2.0	206.9	500 ± 30
303	14.3 ± 0.3	−81.3 ± 1.2	175.9	
313	10.3 ± 0.1	−75.0 ± 0.27	137.3	98 ± 5
320	6.1 ± 0.1	−73.2 ± 1.1	83.3	

[a] Gibbs free energy (ΔG_0) and volume difference (ΔV) at 0.1 MPa calculated by fitting the experimental data to Eq. (7).
[b] Pressure at the midpoint of the transition between native and unfolded state ($f_U = f_N$ and $\Delta G = 0$) calculated by $p_m = \Delta G_0 / \Delta V$.
[c] Trp48 phosphorescence lifetime (τ) measured at 0.1 MPa.

3.3. Pressure-induced unfolding as monitored by Trp48 phosphorescence

The application of high pressure affects the phosphorescence intensity and lifetime of F29A azurin. When the protein unfolds, the phosphorescence lifetime (τ) falls below the detection limit of the instrument and consequently the denatured fraction does not contribute to the phosphorescence emission of the sample. Thus, the intensity of phosphorescence extrapolated to time zero, P_0, when normalized by the prompt fluorescence F, P_0 / F, is a direct measure of the native fraction of the protein population. The pressure profile of P_0 / F was found to be practically identical, within the 5% precision of these measurements, to the fraction of azurin in the native state, $f_N = 1 - f_U$, as determined from the λ_{av} profiles (Fig. 2). This good correspondence between the native fraction of azurin determined by P_0 / F and the fluorescence spectral shift suggests that the macromolecule is either fully native, with long-lived phosphorescence, or completely unfolded. Hence, even at denaturing pressures, there is no evidence of intermediate that could be too flexible to be phosphorescent and with Trp48 still shielded from the solvent to fluoresce to blue. The above correspondence between independent monitors of azurin denaturation supports the validity of a two-state unfolding equilibrium, which means that unfolding proceeds from a compact and still phosphorescent state.

The phosphorescence decay of F29A azurin in fluid solution, such as the WT emission, is uniform and well represented by a single lifetime (Fig. 5A). The pressure dependence at 5, 20 and 40 °C of the F29A azurin phosphorescence lifetime is reported in Fig. 5B. The same figure also reports the trend of the triplet lifetime of WT azurin at 40 °C. Throughout, the pressure modulation of τ was found to be totally elastic, as the change was promptly reversed upon decompression. With pressure, F29A azurin shows an initial increase of τ up to 150 MPa, the trend reverting thereafter with a modest reduction in τ concomitantly with the complete unfolding. At lower temperatures,

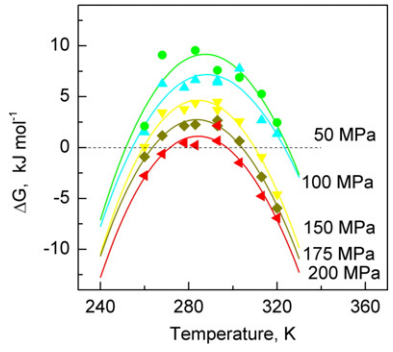

Fig. 3. Temperature dependence of the free energy change of unfolding at various pressures. The solid lines are the best fit of the experimental data to Eq. (8).

Table 2
Pressure dependence of the thermodynamic parameters of F29A azurin for both heat and cold denaturation.

Pressure (MPa)	ΔCp[a] (kJ mol^{-1} K^{-1})	Heat denaturation		Cold denaturation	
		T_m[b] (K)	ΔH_m[c] (kJ mol^{-1})	T_m[b] (K)	ΔH_m[c] (kJ mol^{-1} K^{-1})
50	3.9 ± 1.1	325 ± 4	156 ± 29	252 ± 5	−132 ± 3
100	3.5 ± 0.7	323 ± 3	130 ± 16	254 ± 3	−111 ± 6
150	4.2 ± 0.3	310 ± 1	111 ± 6	259 ± 1	−99 ± 6
175	3.8 ± 0.2	304 ± 1	81 ± 4	264 ± 1	−73 ± 4
200	3.8 ± 0.5	297 ± 2	51 ± 11	271 ± 2	−48 ± 10

[a] Heat capacity change of the unfolding transition.
[b] Temperature at the midpoint of heat and cold denaturation.
[c] Unfolding enthalpy change at T_m.

the lifetime remains practically constant up to about 50 and 200 MPa at 5 °C and 20 °C, respectively, decreasing monotonically at higher pressures.

4. Discussion

The residue Phe29 lies in the β-strand 3 in the protein matrix at 5.1 Å from Trp48 situated in the hydrophobic core of the protein [46]. In theory, the substitution of Phe with Ala should create an empty space of 101 Å^3. Although mutant structures tend to readjust the size of the cavity to attenuate its destabilizing effects, the azurin β-scaffold is very rigid and, consequently, one would expect the relaxation of the structure to be relatively small. In fact, although the mutant shows a lower stability to guanidinium hydrochloride and an increased structural flexibility [25], its native state is almost indistinguishable from the WT protein, as probed by ultraviolet circular dichroism spectroscopy (supplementary information, Fig. 1S).

We used a relatively simple thermodynamic model to analyze the fluorescence measurements and to determine differential changes in the thermodynamic quantities when the protein goes transition from the folded to the unfolded state. In order to evaluate the effect of the mutation on the stability of azurin, we compared the free energy of the pressure unfolding of F29A (Table 1) with those of WT and other cavity-creating mutant forms, F110S and I7S [39]. With respect to WT azurin, at 40 °C, the F29A mutant showed $\Delta\Delta G_0 \cong 26$ kJ mol^{-1}. I7S and F110S azurin mutants showed a similar change ($\Delta\Delta G_0 \cong 27$ kJ mol^{-1}) [39]. From F110S and I7S to F29A, the created cavity shifted from the inner shell to just outside the core of the protein. Unlike what might have been expected, our results indicate that the insertion of cavities penalizes in a similar way protein stability toward pressure, even when moving toward the protein surface. The cost of creating a cavity derives mostly from the missing van der Waals interactions between the side chain to be replaced and the surrounding atoms in the native structure. This energetic cost is estimated at 0.092 kJ mol^{-1} Å^{-3} [17,47], a value frequently used in studies predicting protein stability

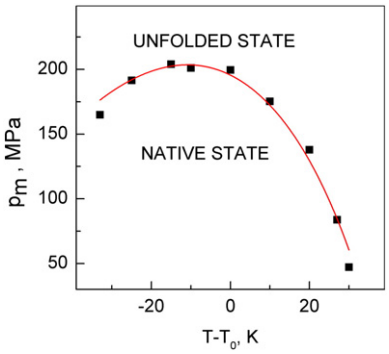

Fig. 4. Pressure–temperature stability diagram of F29A. The solid line is the best fit of the experimental data to Eq. (9) and represents the profile of $\Delta G = 0$. $T_0 = 293$ K.

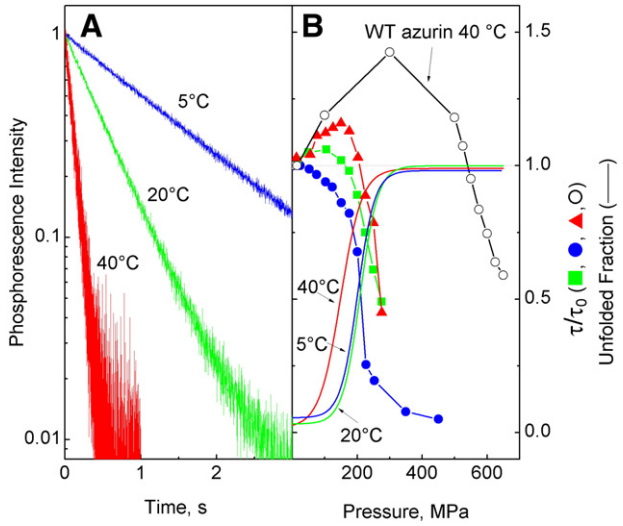

Fig. 5. Pressure induced changes in flexibility and degree of unfolding of F29A azurin at various temperatures. (A) Phosphorescence decay measured at atmospheric pressure at three selected temperatures. (B) Pressure induced unfolding profiles as obtained by fitting the fluorescence data to Eq. (7) (solid lines) and pressure dependence of the phosphorescence lifetime normalized for its value at atmospheric pressure, τ/τ_0. (▲, 40 °C; ■, 20 °C; ●, 5 °C). The pressure dependence of the normalized phosphorescence lifetime of WT azurin at 40 °C is shown for comparison (open circles). Other experimental conditions are as shown in Fig. 1.

[18,48]. This relationship between ΔΔG and ΔV has been found to hold in some cases [23,49], but contrasting data are also available [18,50–52]. In the case of F29A, as previously found for F110S and I7S, the measured ΔΔG value is fairly close to that predicted considering the creation of a cavity of the dimension theoretically calculated from the substitution. The conclusion must therefore be that, in the case of azurin, the size of the cavity affects the stability of the macromolecule more than its position within the protein structure.

The profile of the free energy difference between the native and denatured states plotted against temperature has a convex feature at all pressures (Fig. 3), thus enabling the thermodynamic parameters of both heat and cold denaturation to be characterized. Analysis of the curves shows that the value of ΔC_p is positive and seems to be pressure independent. A single ΔC_p value covers both the cold and the heat denaturation ranges, thus indicating that cold and heat denatured states belong to a single state of the protein. Since the major contribution to the change in volume on unfolding is the elimination of internal voids upon the disruption of the folded structure, introducing an additional cavity, if empty, should increase the value of ΔV by roughly the same amount as the cavity volume. ΔV of F29A unfolding differs by only 15 ml mol^{-1} from that of WT azurin (calculated at 40 °C [39]), a much lower value than theoretically expected from the creation of a cavity due to replacing phenylalanine with alanine. The same discrepancy has been observed with F110S and I7S azurin, for which it was inferred that the cavities were largely filled with water [39]. Although X-ray data are not available, we can assume that, also for the F29A mutant, the cavity created is not empty. It has been hypothesized [3,24] that cavities introduced closer to the protein surface contribute less to the ΔV because of the possibility of direct interaction with the bulk water and/or the tendency of the protein structure to collapse. Notably for F29A azurin, we found the same ΔΔV reported for other cavity azurin mutants where the space was inserted in the inner core of the protein.

Generally in proteins, ΔV of unfolding increases with temperature and can become positive at higher T [43–45,53–55]. A noticeable finding of these experiments was the non-strictly linear behavior of the unfolding ΔV versus temperature. Up to 20 °C, ΔV seems to decrease as temperature increases whereas, above 20 °C, ΔV increases. Despite the relatively large error in determining ΔV, the experimental data suggest

that the expansion of the native state of the protein is wide in the low temperature range, while the expansion of the unfolded form is predominant above 20 °C. Recently it has been proposed that, while hydration plays a significant role in the volumetric properties of unfolded states, void volumes and their tendency to expand with increasing temperature largely determine the volumetric properties of native proteins [3]. The capacity of the protein to expand will depend on the strength of the interactions. Azurin is a very compact protein as revealed by the X-ray structure [46,56] and acrylamide quenching experiments [57,58]. The high β-sheet content provides stiffness for large regions of the protein. However, in spite of its stiffness, in a molecular dynamics simulation study [59] it was shown that the β-barrel of azurin is able to dynamically rearrange its structure and to expand at increasing temperature. Experimentally, the large possibility of the thermal expansion of folded azurin has been verified by measuring the C112S mutant which exhibits a negative difference in thermal expansivity up to 62 °C (paper submitted). In the case of F29A azurin, the positive value of $\Delta\alpha$ above 20 °C suggests that the introduction of a cavity lowers the packing density of the protein structure, reducing the capacity of the native state to further expand with temperature.

4.1. Effects of pressure on protein dynamics

In azurin Trp48, the phosphorescence probe, is located roughly at the center of the β-barrel, the indole ring being surrounded by non-polar side chains that form a compact hydrophobic core [46,56]. Due to the rigid environment, Trp48 exhibits a long phosphorescence lifetime at ambient temperature ($\tau = 0.63$ s) which, translated into local "viscosity", gives $\eta = 5 \times 10^4$ cP [60]. The application of high pressure affects the lifetime of azurin. From the correlation between τ and the fluidity of the chromophore's environment [60,61], the pressure profile of τ of WT azurin at 40 °C indicates an initial tightening of the protein core, presumably owing to the predominance of cavity reduction. The progressive loosening of protein structure in the higher pressure range reflects internal hydration. The creation of a cavity, either empty or filled with water, was expected to enhance local structural fluctuations. In mutants where cavities are created inside the azurin inner core, pressure-induced compaction of the macromolecule is almost or entirely abolished with respect to WT azurin, and protein flexibility increases at lower pressure values [39].

The substitution of Phe29 with Ala affected the lifetime of F29A, which decreased up to 1.2-fold at 40 °C (Table 1) with respect to WT azurin. The gain in flexibility of the cavity mutant, as reported by the decrease in phosphorescence lifetime, may be due to the presence of free voids or to the lubricating action of internal water pools. In the former case the macromolecule would be highly compressible and the pressure drastically would reduce structural fluctuation. In fact, for F29A at 40 °C compaction reaches a maximum at a much lower pressure than WT azurin, the trend reverting thereafter. The lack of or a decreased compaction of the cavity mutant with applied pressure reveals that the cavity is already filled with water, a finding that is consistent with the small variance in ΔV when compared to WT azurin. The ring of Phe29 is partially exposed to the solvent. Its substitution with Ala presumably opens a cleft inside the protein matrix, as indicated by acrylamide quenching experiments [25]. This cleft can thus facilitate water penetration into the protein structure. At lower temperatures, where hydration is favored, the phosphorescence lifetime reports an enhancement of protein flexibility at relatively low pressure, consistent with an overwhelming effect of internal protein hydration over any compaction of the structure. A similar behavior was also observed for the WT azurin when approaching freezing temperatures, where protein hydration is the dominant reaction to pressurization [62]. It appears that the engineered cavity of F29A is largely hydrated and that such a configuration confers high plasticity to the native state even at relatively low pressure. This result is similar to those obtained with F110S and I7S azurin mutants [39]. Thus a cavity engineered in a looser packing site, closer to the protein surface, would seem to lead to an extensive structural rearrangement and facilitate hydration around Trp48 such as cavities inserted in the tight inner core. These data thus highlight that in azurin the distance of the created cavity from the core is not relevant either for the pressure sensitivity of the globular structure or the change in the unfolding volume.

Supplementary data to this article can be found online at http://dx.doi.org/10.1016/j.bpc.2013.06.005.

Acknowledgments

The authors are grateful to Gianluca Presciuttini and Alessandro Puntoni for their valuable technical input.

References

[1] G. Hummer, S. Garde, A.E. Garcia, M.E. Paulaitis, L.R. Pratt, The pressure dependence of hydrophobic interactions is consistent with the observed pressure denaturation of proteins, Proceedings of the National Academy of Sciences of the United States of America 95 (1998) 1552–1555.
[2] J.B. Rouget, T. Aksel, J. Roche, J.L. Saldana, A.E. Garcia, D. Barrick, C.A. Royer, Size and sequence and the volume change of protein folding, Journal of the American Chemical Society 133 (2011) 6020–6027.
[3] J. Roche, J.A. Caro, D.R. Norberto, P. Barthe, C. Roumestand, J.L. Schlessman, A.E. Garcia, B.E. Garcia-Moreno, C.A. Royer, Cavities determine the pressure unfolding of proteins, Proceedings of the National Academy of Sciences of the United States of America 109 (2012) 6945–6950.
[4] S. Sonavane, P. Chakrabarti, Cavities and atomic packing in protein structures and interfaces, PLoS Computational Biology 4 (2008) e1000188.
[5] B.P. Schoenborn, H.C. Watson, J.C. Kendrew, Binding of xenon to sperm whale myoglobin, Nature 207 (1965) 28–30.
[6] B.P. Schoenborn, Binding of xenon to horse haemoglobin, Nature 208 (1965) 760–762.
[7] R.F. Tilton Jr., I.D. Kuntz Jr., G.A. Petsko, Cavities in proteins: structure of a metmyoglobin–xenon complex solved to 1.9 A, Biochemistry 23 (1984) 2849–2857.
[8] R.K. Wierenga, M.E. Noble, R.C. Davenport, Comparison of the refined crystal structures of liganded and unliganded chicken, yeast and trypanosomal triosephosphate isomerase, Journal of Molecular Biology 224 (1992) 1115–1126.
[9] B. Lee, F.M. Richards, The interpretation of protein structures: estimation of static accessibility, Journal of Molecular Biology 55 (1971) 379–400.
[10] A.A. Rashin, M. Iofin, B. Honig, Internal cavities and buried waters in globular proteins, Biochemistry 25 (1986) 3619–3625.
[11] R.F. Tilton Jr., U.C. Singh, S.J. Weiner, M.L. Connolly, I.D. Kuntz Jr., P.A. Kollman, N. Max, D.A. Case, Computational studies of the interaction of myoglobin and xenon, Journal of Molecular Biology 192 (1986) 443–456.
[12] D.G. Lambright, S. Balasubramanian, S.M. Decatur, S.G. Boxer, Anatomy and dynamics of a ligand-binding pathway in myoglobin: the roles of residues 45, 60, 64, and 68, Biochemistry 33 (1994) 5518–5525.
[13] C. Lee, S.H. Park, M.Y. Lee, M.H. Yu, Regulation of protein function by native metastability, Proceedings of the National Academy of Sciences of the United States of America 97 (2000) 7727–7731.
[14] M. Karpusas, W.A. Baase, M. Matsumura, B.W. Matthews, Hydrophobic packing in T4 lysozyme probed by cavity-filling mutants, Proceedings of the National Academy of Sciences of the United States of America 86 (1989) 8237–8241.
[15] J.T. Kellis Jr., K. Nyberg, A.R. Fersht, Energetics of complementary side-chain packing in a protein hydrophobic core, Biochemistry 28 (1989) 4914–4922.
[16] A.E. Eriksson, W.A. Baase, J.A. Wozniak, B.W. Matthews, A cavity-containing mutant of T4 lysozyme is stabilized by buried benzene, Nature 355 (1992) 371–373.
[17] A.E. Eriksson, W.A. Baase, X.J. Zhang, D.W. Heinz, M. Blaber, E.P. Baldwin, B.W. Matthews, Response of a protein structure to cavity-creating mutations and its relation to the hydrophobic effect, Science 255 (1992) 178–183.
[18] D.H. Adamek, L. Guerrero, M. Blaber, D.L. Caspar, Structural and energetic consequences of mutations in a solvated hydrophobic cavity, Journal of Molecular Biology 346 (2005) 307–318.
[19] J.A. Ernst, R.T. Clubb, H.X. Zhou, A.M. Gronenborn, G.M. Clore, Demonstration of positionally disordered water within a protein hydrophobic cavity by NMR, Science 267 (1995) 1813–1817.
[20] B.W. Matthews, Structural and genetic analysis of protein stability, Annual Review of Biochemistry 62 (1993) 139–160.
[21] B.W. Matthews, A.G. Morton, F.W. Dahlquist, Use of NMR to detect water within nonpolar protein cavities, Science 270 (1995) 1847–1849.
[22] M.L. Quillin, W.A. Breyer, I.J. Griswold, B.W. Matthews, Size versus polarizability in protein–ligand interactions: binding of noble gases within engineered cavities in phage T4 lysozyme, Journal of Molecular Biology 302 (2000) 955–977.
[23] A.M. Buckle, P. Cramer, A.R. Fersht, Structural and energetic responses to cavity-creating mutations in hydrophobic cores: observation of a buried water molecule and the hydrophilic nature of such hydrophobic cavities, Biochemistry 35 (1996) 4298–4305.
[24] B.W. Matthews, Proteins under pressure, Proceedings of the National Academy of Sciences of the United States of America 109 (2012) 6792–6793.

[25] E. Gabellieri, E. Balestreri, A. Galli, P. Cioni, Cavity-creating mutations in *Pseudomonas aeruginosa* azurin: effects on protein dynamics and stability, Biophysical Journal 95 (2008) 771–781.
[26] P. Cioni, G.B. Strambini, Tryptophan phosphorescence and pressure effects on protein structure, Biochimica et Biophysica Acta-Protein Structure and Molecular Enzymology 1595 (2002) 116–130.
[27] G.B. Strambini, E. Gabellieri, Phosphorescence from Trp-48 in azurin — influence of Cu(II), Cu(I), Ag(I), and Cd(II) at the coordination site, Journal of Physical Chemistry 95 (1991) 4352–4356.
[28] G.B. Strambini, E. Gabellieri, Proteins in frozen solutions: evidence of ice-induced partial unfolding, Biophysical Journal 70 (1996) 971–976.
[29] G.B. Strambini, E. Gabellieri, Intrinsic phosphorescence from proteins in the solid state, Photochemistry and Photobiology 39 (1984) 725–729.
[30] P. Cioni, E. Gabellieri, Protein dynamics and pressure: what can high pressure tell us about protein structural flexibility? Biochimica et Biophysica Acta 1814 (2011) 934–941.
[31] P. Cioni, E. Bramanti, G.B. Strambini, Effects of sucrose on the internal dynamics of azurin, Biophysical Journal 88 (2005) 4213–4222.
[32] J.E. Hansen, D.G. Steel, A. Gafni, Detection of a pH-dependent conformational change in azurin by time-resolved phosphorescence, Biophysical Journal 71 (1996) 2138–2143.
[33] G.W. Canters, The azurin gene from *Pseudomonas aeruginosa* codes for a pre-protein with a signal peptide. Cloning and sequencing of the azurin gene, FEBS Letters 212 (1987) 168–172.
[34] M. van de Kamp, M.C. Silvestrini, M. Brunori, J. Van Beeumen, F.C. Hali, G.W. Canters, Involvement of the hydrophobic patch of azurin in the electron-transfer reactions with cytochrome C551 and nitrite reductase, European Journal of Biochemistry 194 (1990) 109–118.
[35] M. van de Kamp, F.C. Hali, N. Rosato, A.F. Agro, G.W. Canters, Purification and characterization of a non-reconstitutable azurin, obtained by heterologous expression of the *Pseudomonas aeruginosa* azu gene in *Escherichia coli*, Biochimica et Biophysica Acta 1019 (1990) 283–292.
[36] J.V. Mersol, D.G. Steel, A. Gafni, Detection of intermediate protein conformations by room-temperature tryptophan phosphorescence spectroscopy during de-naturation of *Escherichia coli* alkaline-phosphatase, Biophysical Chemistry 48 (1993) 281–291.
[37] A. Maeno, H. Matsuo, K. Akasaka, The pressure–temperature phase diagram of hen lysozyme at low pH, Biophysics 5 (2009) 1–9.
[38] S.A. Hawley, Reversible pressure–temperature denaturation of chymotrypsinogen, Biochemistry 10 (1971) 2436–2442.
[39] P. Cioni, Role of protein cavities on unfolding volume change and on internal dynamics under pressure, Biophysical Journal 91 (2006) 3390–3396.
[40] A.A. Zamyatnin, Protein volume in solution, Progress in Biophysics and Molecular Biology 24 (1972) 107–123.
[41] D.P. Kharakoz, Volumetric properties of proteins and their analogs in diluted water solutions. 1. Partial volumes of amino acids at 15–55 °C, Biophysical Chemistry 34 (1989) 115–125.
[42] M. Kikuchi, M. Sakurai, K. Nitta, Partial molar volumes and adiabatic compress-ibilities of amino acids in dilute aqueous solutions at 5, 15, 25, 35, and 45 °C, Journal of Chemical & Engineering Data 40 (1995) 935–942.
[43] M.W. Lassalle, H. Yamada, K. Akasaka, The pressure–temperature free energy-landscape of staphylococcal nuclease monitored by ^{1}H NMR, Journal of Molecular Biology 298 (2000) 293–302.
[44] A. Zipp, W. Kauzmann, Pressure denaturation of metmyoglobin, Biochemistry 12 (1973) 4217–4228.
[45] J.F. Brandts, R.J. Oliveira, C. Westort, Thermodynamics of protein denaturation. Effect of pressu on the denaturation of ribonuclease A, Biochemistry 9 (1970) 1038–1047.
[46] H. Nar, A. Messerschmidt, R. Huber, M. van de Kamp, G.W. Canters, Crystal structure analysis of oxidized Pseudomonas aeruginosa azurin at pH 5.5 and pH 9.0. A pH-induced conformational transition involves a peptide bond flip, Journal of Molecular Biology 221 (1991) 765–772.
[47] J. Xu, W.A. Baase, E. Baldwin, B.W. Matthews, The response of T4 lysozyme to large-to-small substitutions within the core and its relation to the hydrophobic effect, Protein Science 7 (1998) 158–177.
[48] S.J. Hubbard, K.H. Gross, P. Argos, Intramolecular cavities in globular proteins, Protein Engineering 7 (1994) 613–626.
[49] K. Takano, K. Ogasahara, H. Kaneda, Y. Yamagata, S. Fujii, E. Kanaya, M. Kikuchi, M. Oobatake, K. Yutani, Contribution of hydrophobic residues to the stability of human lysozyme: calorimetric studies and X-ray structural analysis of the five isoleucine to valine mutants, Journal of Molecular Biology 254 (1995) 62–76.
[50] A.M. Buckle, K. Henrick, A.R. Fersht, Crystal structural analysis of mutations in the hydrophobic cores of barnase, Journal of Molecular Biology 234 (1993) 847–860.
[51] G.S. Ratnaparkhi, R. Varadarajan, Thermodynamic and structural studies of cavity formation in proteins suggest that loss of packing interactions rather than the hydrophobic effect dominates the observed energetics, Biochemistry 39 (2000) 12365–12374.
[52] M. Vlassi, G. Cesareni, M. Kokkinidis, A correlation between the loss of hydrophobic core packing interactions and protein stability, Journal of Molecular Biology 285 (1999) 817–827.
[53] G. Panick, R. Malessa, R. Winter, G. Rapp, K.J. Frye, C.A. Royer, Structural char-acterization of the pressure-denatured state and unfolding/refolding kinetics of staphylococcal nuclease by synchrotron small-angle X-ray scattering and Fourier-transform infrared spectroscopy, Journal of Molecular Biology 275 (1998) 389–402.
[54] G. Panick, G.J. Vidugiris, R. Malessa, G. Rapp, R. Winter, C.A. Royer, Exploring the temperature–pressure phase diagram of staphylococcal nuclease, Biochemistry 38 (1999) 4157–4164.
[55] C.A. Royer, Revisiting volume changes in pressure-induced protein unfolding, Biochimica et Biophysica Acta 1595 (2002) 201–209.
[56] H. Nar, A. Messerschmidt, R. Huber, M. van de Kamp, G.W. Canters, Crystal structure of *Pseudomonas aeruginosa* apo-azurin at 1.85 A resolution, FEBS Letters 306 (1992) 119–124.
[57] P. Cioni, G.B. Strambini, Acrylamide quenching of protein phosphorescence as a monitor of structural fluctuations in the globular fold, Journal of the American Chemical Society 120 (1998) 11749–11757.
[58] G.B. Strambini, M. Gonnelli, Amplitude spectrum of structural fluctuations in proteins from the internal diffusion of solutes of increasing molecular size: a Trp phosphorescence quenching study, Biochemistry 50 (2011) 970–980.
[59] B. Rizzuti, L. Sportelli, R. Guzzi, Structural, dynamical and functional aspects of the inner motions in the blue copper protein azurin, Biophysical Chemistry 125 (2007) 532–539.
[60] G.B. Strambini, M. Gonnelli, Tryptophan phosphorescence in fluid solution, Journal of the American Chemical Society 117 (1995) 7646–7651.
[61] M. Gonnelli, G.B. Strambini, Phosphorescence lifetime of tryptophan in proteins, Biochemistry 34 (1995) 13847–13857.
[62] P. Cioni, G.B. Strambini, Pressure/temperature effects on protein flexibility from acrylamide quenching of protein phosphorescence, Journal of Molecular Biology 291 (1999) 955–964.